Channel Estimation for Non-Stationary Extremely Large-Scale MIMO

Yuhao Chen, Zijian Zhang, Mingyao Cui, and Linglong Dai, *Fellow*, *IEEE*
Department of Electronic Engineering, Tsinghua University, Beijing 100084, China
Beijing National Research Center for Information Science and Technology, Beijing 100084, China
E-mail: {chen-yh21, zhangzj20, cmy20}@mails.tsinghua.edu.cn, daill@tsinghua.edu.cn

2023 IEEE 97th Vehicular Technology Conference (VTC2023-Spring) | 979-8-3503-1114-3/23/$31.00 ©2023 IEEE | DOI: 10.1109/VTC2023-Spring57618.2023.10199467

***Abstract*—Extremely large-scale multiple-input multiple-output (XL-MIMO) is a promising technology for future 6G communications. To realize effective precoding, channel estimation schemes are essential to acquire precise channel state information (CSI), while most existing schemes work relying on the spatial stationary assumption. In XL-MIMO systems, however, the spatial non-stationary effect naturally exists. Such effect can hardly be recognized by existing channel estimation schemes, leading to a severe accuracy loss of channel estimation. To address this problem, in this paper, we study the spatial non-stationary channel estimation for XL-MIMO systems. Specifically, we propose a group time block code (GTBC) based signal extraction scheme. The key idea is to artificially create and exploit the time-domain relevance of non-stationary effect, which allows XL-MIMO to recognize such effect in the space domain. In this way, the spatial non-stationary channel is converted to a series of spatial stationary channels. To effectively estimate these channels, a GTBC-based polar-domain simultaneous orthogonal matching pursuit (GP-SOMP) algorithm is proposed as a solution. Simulation results reveal that the proposed GP-SOMP algorithm can recognize the spatial non-stationary effect in XL-MIMO systems and realize a much more accurate channel estimation than existing schemes.**

I. Introduction

Extremely large-scale multiple-input multiple-output (XL-MIMO) at millimeter-wave (mmWave) or terahertz (THz) is envisioned as a key technology of six-generation (6G) networks, thanks to its strengths in high spectrum efficiency, abundant bandwidth resources, and so forth [1], [2]. Considering the high-power radio-frequency (RF) chain in high-frequency communications [3], hybrid precoding architecture is widely utilized for high-frequency XL-MIMO [4], [5]. To perform efficient hybrid precoding, accurate channel state information (CSI) with low pilot overhead is of great importance, especially for XL-MIMO hybrid precoding equipped with a larger number of antennas but a few RF chains.

To reduce the pilot overhead in channel estimation, several compressive sensing (CS) based schemes have been studied [6]–[9] by exploiting the sparse structure of high-frequency wireless channels. Most of these schemes rely on the spatial stationary assumption, which means that the entire array sees the same scatterers and users. In XL-MIMO systems, however, the impact of spatial non-stationary effect is particularly significant, leading to different regions of the array may see totally different scatterers or users. Existing schemes mostly neglect this effect, so the sparse representation of the whole channel is consistent. Actually, this is not the case in a spatial non-stationary channel, where the sparse representations of different channel parts are inconsistent. Consequently, such effect brings a severe mismatch between the sparse representation of existing CS based channel estimation schemes and the actual XL-MIMO channels. If existing schemes are directly utilized, the spatial non-stationary effect cannot be captured and the channel estimation accuracy will be quite low.

To handle the spatial non-stationarity in XL-MIMO systems, some recent attempts have been made [10]–[12], which are based on the assumption that although the whole channel is spatial non-stationary, the sub-channel corresponding to a part of the antenna array (i.e., a sub-array) can be treated as spatial stationary, which is also verified by the measurement in [13]. However, all these spatial non-stationary solutions are based on a full digital precoding structure, so the received signals of different sub-arrays can be independently analyzed. In practical hybrid precoding systems, these schemes cannot work anymore since the received signals of a large number of antennas are mixed together and the received signals from different sub-arrays cannot be decoupled. To the best of our knowledge, there have not been a proper solution to the non-stationary channel estimation problem in XL-MIMO systems with hybrid precoding.

To fill in this gap, in this paper, we study the spatial non-stationary channel estimation for both far-field and near-field electromagnetic environments in practical XL-MIMO systems. Specifically, inspired by the classical Alamouti code, we propose a group time block code (GTBC) based signal extraction scheme to decouple the mixed signals of all antennas. The key idea is to artificially create and exploit the time-domain relevance of non-stationary effect, which allows XL-MIMO to recognize such effect in the space domain. In this way, the spatial non-stationary channel is converted to a series of spatial stationary channels. With the proposed GTBC based signal extraction scheme, a GTBC-based polar-domain simultaneous orthogonal matching pursuit (GP-SOMP) algorithm is proposed to estimate the spatial non-stationary channel efficiently. Simulation results reveal that the proposed GP-SOMP algorithm can recognize the spatial non-stationary effect in XL-MIMO systems and realize a much more accurate channel estimation than existing schemes.

The rest of this paper is organized as follows. In Section II, the system model is introduced, where the spherical wave propagation effects and the spatial non-stationary effects in XL-MIMO systems are elaborated. In Section III, the GTBC based signal extraction scheme is proposed. In Section IV, the GP-SOMP algorithm is proposed. Simulations are carried out Section V, and finally conclusions are drawn in Section VI.

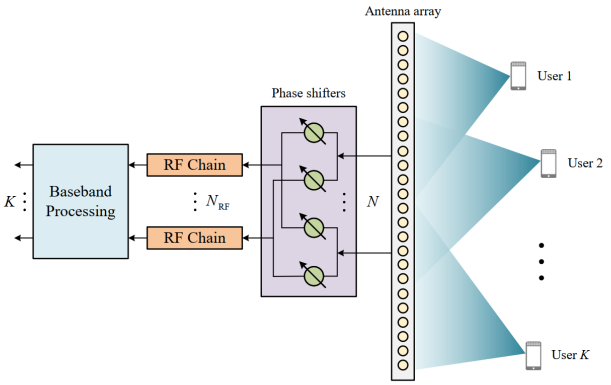

Fig. 1. XL-MIMO system with hybrid precoding

II. System Model

An uplink time division duplexing (TDD) based XL-MIMO communication system is considered in this paper, as illustrated in Fig. 1. The base station (BS) employs a fully connected hybrid precoding architecture with N_{RF} radio frequency (RF) chains and an N-antenna uniform linear array (ULA). The antenna spacing of the ULA is $d = \frac{c}{2f_c}$, where f_c represents the central frequency. K users equipped with single-antennas are served with M subcarriers simultaneously. During channel estimation stage, orthogonal pilot sequences are widely utilized [14], in the following discussion, we only consider an arbitrary user for uplink channel estimation.

Specifically, we denote $s_{m,p}$ as the transmit pilot in time slot p at the m-th subcarrier. Then, the pilot $\mathbf{y}_{m,p} \in \mathbb{C}^{N_{\mathrm{RF}} \times 1}$ received by the BS can be represented as

$$\mathbf{y}_{m,p} = \mathbf{A}_p \mathbf{h}_m s_{m,p} + \mathbf{A}_p \mathbf{n}_{m,p}, \tag{1}$$

where $\mathbf{A}_p \in \mathbb{C}^{N_{\mathrm{RF}} \times N}$ is the analog combining matrix satisfying the constant modulus constraint $|\mathbf{A}_p(i,j)| = \frac{1}{\sqrt{N}}$, $\mathbf{n}_{m,p} \in \mathbb{C}^{N \times 1}$ is the Gaussian complex noise following the distribution $\mathcal{CN}\left(0, \sigma^2 \mathbf{I}_N\right)$ with σ^2 being the noise power. We define the pilot length as P and assume that $s_{m,p} = 1$ for all $p = 1, 2, ..., P$. Then the overall received pilots at the m-th subcarrier $\mathbf{y}_m = \left[\mathbf{y}_{m,1}^T, ..., \mathbf{y}_{m,P}^T\right]^T \in \mathbb{C}^{PN_{\mathrm{RF}} \times 1}$ can be represented as

$$\mathbf{y}_m = \mathbf{A}\mathbf{h}_m + \mathbf{n}_m, \tag{2}$$

where $\mathbf{A} = \left[\mathbf{A}_1^T, ..., \mathbf{A}_P^T\right]^T \in \mathbb{C}^{PN_{\mathrm{RF}} \times N}$ denotes the overall observation matrix, where the elements in $\mathbf{A}$ are independent and randomly generated from the set $\mathbb{H} = \frac{1}{\sqrt{N}}\{-1, 1\}$, $\mathbf{n}_m = \left[\mathbf{n}_{m,1}^T \mathbf{A}_1^T, ..., \mathbf{n}_{m,P}^T \mathbf{A}_P^T\right]^T \in \mathbb{C}^{PN_{\mathrm{RF}} \times 1}$ denotes the effective noise.

As XL-MIMO has a pretty large array aperture, its near-field range could be dozens of or even hundreds of meters [15]. Therefore, we need to use the spherical wave propagation model to represent the wireless channels as

$$\tilde{\mathbf{h}}_m = \sqrt{\frac{N}{L}} \sum_{\ell=1}^{L} g_\ell e^{-jk_m r_\ell} \mathbf{b}(\theta_\ell, r_\ell), \tag{3}$$

where $k_m = \frac{2\pi f_m}{c}$ denotes the wave number, L denotes the total number of paths, and $g_\ell, r_\ell, \theta_\ell$ denote the complex path gain, the distance and the angle of the ℓ-th path, respectively. It is worth noting that the steering vector $\mathbf{b}(\cdot)$ is dependent on both the angle θ_l and the distance r_l related not only to the angle θ_ℓ, but also to the distance r_ℓ. Specifically, the steering vector $\mathbf{b}$ can be represented as

$$\mathbf{b}(\theta_\ell, r_\ell) = \frac{1}{\sqrt{N}} \left[e^{-jk_c\left(r_\ell^{(1)} - r_\ell\right)}, ..., e^{-jk_c\left(r_\ell^{(N)} - r_\ell\right)}\right]^T, \tag{4}$$

where $k_c = \frac{2\pi}{\lambda_c}$ denotes the wave number of the central subcarrier and $r_\ell^{(n)}$ denotes the distance between the n-th BS antenna and the l-th scatter, which is formulated as

$$r_\ell^{(n)} = \sqrt{r_\ell^2 - 2r_\ell \delta_n d\theta_\ell + \delta_n^2 d^2}, \tag{5}$$

with $\delta_n = \frac{2n-N-1}{2}, n = 1, 2, ..., N$.

Apart from the near-field effect, the large array aperture also brings the spatial non-stationary effect, making different antennas visible to different scatterers or users, which is described by separated visibility regions (VRs). Taking the VR of each path into account, the channel model in (3) should be modified as

$$\mathbf{h}_m = \sqrt{\frac{N}{L}} \sum_{\ell=1}^{L} g_\ell e^{-jk_m r_\ell} \mathbf{b}(\theta_\ell, r_\ell) \odot \mathbf{v}(\Upsilon_\ell), \tag{6}$$

where Υ_ℓ contains the indexes of antennas visible to the ℓ-th scatter, and $\mathbf{v}(\Upsilon_\ell)$ is the mask vector indexed by Υ_ℓ. Specifically, the n-th element of $\mathbf{v}(\Upsilon_\ell)$ is defined as

$$[\mathbf{v}(\Upsilon_\ell)]_n = \begin{cases} 1, & n \in \Upsilon_\ell, \\ 0, & n \notin \Upsilon_\ell. \end{cases} \tag{7}$$

As shown in [13], though the entire channel is spatial non-stationary, the sub-channels correponding to a part of the array (i. e. a sub-array) can be seen as spatial stationary. Considering a XL-MIMO divided into N_s smaller sub-arrays, without loss of generality, we assume that $\frac{N}{N_s}$ is an integer. The set $\tilde{\Upsilon}_\ell$ is introduced to index the sub-arrays that can see the ℓ-th scatter, which is represented as

$$\tilde{\Upsilon}_\ell = \{n_{s,1}, ..., n_{s,L}\}, \tag{8}$$

where $1 \le n_{s,i} \le N_s$ denotes the index of sub-array. Then, (7) can be further given by

$$[\mathbf{v}(\Upsilon_\ell)]_n = \begin{cases} 1, & \left\lceil \frac{nN_s}{N} \right\rceil \in \tilde{\Upsilon}_\ell, \\ 0, & \text{else.} \end{cases} \tag{9}$$

The target of this paper is to estimate $\mathbf{h}_m$ from $\mathbf{y}_m$ by exploiting the non-stationary structure of $\mathbf{h}_m$.

III. Proposed GTBC based Signal Extraction Scheme

In this section, we propose a group time block code (GTBC) based signal extraction scheme to extract the received signal corresponding to each sub-array from the mixed signals of all antennas in XL-MIMO hybrid precoding systems. Inspired

$$\tilde{\mathbf{\Lambda}}_{N_s} = \begin{bmatrix} \mathbf{1}_{1\times N/N_s} \times \mathbf{\Lambda}_{N_s}[1,1] & \mathbf{1}_{1\times N/N_s} \times \mathbf{\Lambda}_{N_s}[1,2] & \cdots & \mathbf{1}_{1\times N/N_s} \times \mathbf{\Lambda}_{N_s}[1,N_s] \\ \mathbf{1}_{1\times N/N_s} \times \mathbf{\Lambda}_{N_s}[2,1] & \mathbf{1}_{1\times N/N_s} \times \mathbf{\Lambda}_{N_s}[2,2] & \cdots & \mathbf{1}_{1\times N/N_s} \times \mathbf{\Lambda}_{N_s}[2,N_s] \\ \vdots & \vdots & \ddots & \vdots \\ \mathbf{1}_{1\times N/N_s} \times \mathbf{\Lambda}_{N_s}[N_s,1] & \mathbf{1}_{1\times N/N_s} \times \mathbf{\Lambda}_{N_s}[N_s,2] & \cdots & \mathbf{1}_{1\times N/N_s} \times \mathbf{\Lambda}_{N_s}[N_s,N_s] \end{bmatrix} \tag{17}$$

by the classical Alamouti code, in order to obtain the ability to recognize the spatial non-stationary in space domain, we create the relevance in the time domain artificially.

Without loss of generality, we consider the received signal in time slot p at the m-th subcarrier of an arbitrary RF chain, $1 \le i \le N_{\mathrm{RF}}$, which can be formulated as

$$y_{m,p} = \mathbf{A}_p \mathbf{h}_m s_{m,p} + \mathbf{A}_p \mathbf{n}_{m,p}. \tag{10}$$

We start from a simple case, where the XL-MIMO is divided into two sub-arrays. To describe the sub-channels corresponding to the two sub-arrays more clearly, $\mathbf{A}$ and $\mathbf{h}_m$ are divided into two parts and (10) could be rewritten as

$$\begin{aligned} y_{m,p} &= \begin{bmatrix} \mathbf{A}_{p,1} & \mathbf{A}_{p,2} \end{bmatrix} \begin{bmatrix} \mathbf{h}_{m,1} \\ \mathbf{h}_{m,2} \end{bmatrix} s_{m,p} + \mathbf{A}_p \mathbf{n}_{m,p} \\ &= \mathbf{A}_{p,1}\mathbf{h}_{m,1}s_{m,p} + \mathbf{A}_{p,2}\mathbf{h}_{m,2}s_{m,p} + \mathbf{A}_p \mathbf{n}_{m,p}, \end{aligned} \tag{11}$$

where $\mathbf{A}_{p,j}, \mathbf{h}_{m,j}$ denote the combing matrix of the p-th time slot and the channel matrix corresponding to the j-th sub-array, respectively. In traditional channel estimation procedure, for a certain RF chain, the randomly generated analog combing matrix in each time slot merely mix all the received signal of BS antennas, making the received signals of different time slots independent from each other. This makes it challenging to extract the received signal corresponding to each sub-array. In order to acquire the ability to decouple the received signals in the space domain, instead of generating $\mathbf{A}_p$ at each time slot independently, we use GTBC to design $\mathbf{A}_p$ at every two adjacent time slots in order to artificially create the relevance of received signals. To be specific, let $\mathbf{A}_{p+1,1} = \mathbf{A}_{p,1}, \mathbf{A}_{p+1,2} = -\mathbf{A}_{p,2}, s_{m,p+1} = s_{m,p}$, and then the received signal at the $(p+1)$-th time slot becomes

$$y_{m,p+1} = \mathbf{A}_{p,1}\mathbf{h}_{m,1}s_{m,p} - \mathbf{A}_{p,2}\mathbf{h}_{m,2}s_{m,p} + \mathbf{A}_{p+1}\mathbf{n}_{m,p+1}. \tag{12}$$

By combining (11) and (12), the received signals correponding to the two sub-arrays can be decoupled as

$$\begin{cases} \tilde{y}_{m,p,1} = \dfrac{y_{m,p} + y_{m,p+1}}{2} = \mathbf{A}_{p,1}\mathbf{h}_{m,1}s_{m,p} + \tilde{\mathbf{n}}_{m,p,1} \\ \tilde{y}_{m,p,2} = \dfrac{y_{m,p} - y_{m,p+1}}{2} = \mathbf{A}_{p,2}\mathbf{h}_{m,2}s_{m,p} + \tilde{\mathbf{n}}_{m,p,2} \end{cases}, \tag{13}$$

where $\tilde{\mathbf{n}}_{m,p,1} = \frac{\mathbf{A}_p\mathbf{n}_{m,p} + \mathbf{A}_{p+1}\mathbf{n}_{m,p+1}}{2}$, and $\tilde{\mathbf{n}}_{m,p,2} = \frac{\mathbf{A}_p\mathbf{n}_{m,p} - \mathbf{A}_{p+1}\mathbf{n}_{m,p+1}}{2}$. The received signals corresponding to each sub-array are properly extracted.

The above operation in (11) and (12) can be abstracted as

$$\begin{bmatrix} \mathbf{A}_p \\ \mathbf{A}_{p+1} \end{bmatrix} = \begin{bmatrix} \mathbf{A}_{p,1} & \mathbf{A}_{p,2} \\ \mathbf{A}_{p,1} & \mathbf{A}_{p,2} \end{bmatrix} \odot \underbrace{\begin{bmatrix} 1 & 1 \\ 1 & -1 \end{bmatrix}}_{\mathbf{P}} = \begin{bmatrix} \mathbf{A}_{p,1} & \mathbf{A}_{p,2} \\ \mathbf{A}_{p,1} & -\mathbf{A}_{p,2} \end{bmatrix}. \tag{14}$$

Here, the matrix $\mathbf{P}$ is called the GTBC matrix, based on which the combining matrices in every 2 adjacent time slots can be generated by a random basic combining matrix. Correspondingly, the operation in (13) can be abstracted as

$$\begin{bmatrix} \tilde{y}_{m,p,1} \\ \tilde{y}_{m,p,2} \end{bmatrix} = \underbrace{\begin{bmatrix} \frac{1}{2} & \frac{1}{2} \\ \frac{1}{2} & -\frac{1}{2} \end{bmatrix}}_{\mathbf{P}^{-1}} \begin{bmatrix} y_{m,p} \\ y_{m,p+1} \end{bmatrix}. \tag{15}$$

For a more general scenario, where the XL-MIMO is divided into N_s sub-arrays, the design of the GTBC in every N_s adjacent time slots turns to the design of GTBC matrix $\mathbf{P}$. Hadamard matrix provides a proper solution to this problem. Let $\mathbf{\Lambda}_n$ be the n-order Hadamard matrix, whose elements are either 1 or -1. In the above simple case where the XL-MIMO is divided into two sub-arrays, $\mathbf{P} = \mathbf{\Lambda}_2 = \begin{bmatrix} 1 & 1 \\ 1 & -1 \end{bmatrix}$, while the Hadamard matrix with order 2^k can be further derived by

$$\mathbf{\Lambda}_{2^k} = \begin{bmatrix} \mathbf{\Lambda}_{2^{k-1}} & \mathbf{\Lambda}_{2^{k-1}} \\ \mathbf{\Lambda}_{2^{k-1}} & -\mathbf{\Lambda}_{2^{k-1}} \end{bmatrix}. \tag{16}$$

Considering a XL-MIMO system, where the BS is divided into N_s sub-arrays, the adjacent N_s time slots share a common basic combining matrix. We assume that $N_s = 2^k$. To match the dimension of the BS antenna number, the $\mathbf{\Lambda}_{N_s}$ need to be processed as (17), where $\mathbf{1}_{m\times n}$ denotes the all one matrix with dimension $m \times n$.

Taking the p-th time slot to the $(p+N_s-1)$-th time slot as an example, the combining matrix can be generated based on $\mathbf{A}_p$ and the GTBC matrix by

$$\mathbf{A}_{p+i} = \begin{bmatrix} \mathbf{A}_{p,1} & \mathbf{A}_{p,2} & \cdots & \mathbf{A}_{p,N_s} \end{bmatrix} \odot \tilde{\mathbf{\Lambda}}_{N_s}[i,:], \tag{18}$$

where $i = 0, 1, ..., N_s - 1$, $\mathbf{A}_{p,j}$ denotes the $((j-1)N/N_s + 1)$-th column to the (jN/N_s)-th column of $\mathbf{A}_p$. With the help of Hadamard matrix, the combining matrix can be generated based on the GTBC. The designed combining matrix is relevant in the time domain, which is the foundation to extract the received signals corresponding to each sub-array.

After receiving the combined received signal, the received signal corresponding to each sub-array is extracted at the decoding stage based on the GTBC. After the pilot transmission stage, the BS receives P signals, denoted as $y_{m,j}, j = 1, 2, ..., P$. For the i-th pilot transmission sub-frame, the received signals corresponding to each sub-array can be represented as

$$\begin{bmatrix} \tilde{y}_{m,i,1} \\ \vdots \\ \tilde{y}_{m,i,N_s} \end{bmatrix} = \underbrace{\frac{1}{N_s}\mathbf{\Lambda}_{N_s}}_{\mathbf{P}^{-1}} \begin{bmatrix} y_{m,(i-1)N_s+1} \\ \vdots \\ y_{m,iN_s} \end{bmatrix}. \tag{19}$$

Combining all pilot transmission sub-frames, the received signal corresponding to the k-th sub-array can be denoted as $\tilde{\mathbf{y}}_{m,k} = \left[\tilde{y}_{m,1,k}, \tilde{y}_{m,2,k}, ..., \tilde{y}_{m,P/N_s,k}\right], k = 1, 2, ..., N_s$. The corresponding observation matrix can be represented as

$$\mathbf{A}_{\mathrm{sub},k} = \begin{bmatrix} \mathbf{A}_{1,k}^H & \mathbf{A}_{N_s+1,k}^H & \cdots & \mathbf{A}_{P-N_s+1,k}^H \end{bmatrix}^H. \quad (20)$$

Then, the received signal corresponding to the k-th sub-array can be represented as

$$\tilde{\mathbf{y}}_{m,k} = \mathbf{A}_{\mathrm{sub},k}\mathbf{h}_{m,k} + \tilde{\mathbf{n}}_{m,k}, \quad (21)$$

and the received pilots corresponding to each sub-array are extracted.

IV. Proposed Non-stationary Channel Estimation Scheme

Based on the extracted received pilots of each sub-array, the whole spatial non-stationary channel is converted to a series of spatial stationary channels and can be estimated respectively. For a certain user, the received pilot corresponding to the k-th sub-array at the m-th subcarrier can be represented as

$$\tilde{\mathbf{y}}_{m,k} = \mathbf{A}_{\mathrm{sub},k}\mathbf{W}_{N_s}\mathbf{h}_{m,k}^{\mathcal{P}} + \tilde{\mathbf{n}}_{m,k} = \mathbf{\Psi}_k\mathbf{h}_{m,k}^{\mathcal{P}} + \tilde{\mathbf{n}}_{m,k}, \quad (22)$$

where $\mathbf{\Psi}_k = \mathbf{A}_{\mathrm{sub},k}\mathbf{W}_{N_s}$ and $\mathbf{W}_{N_s}$ is the polar-domain transform matrix in [8], which can represent the near-field channel in a sparse way.

In the considered scenario, the bandwidth is small compared to the central frequency, so all subcarriers share the same sparse channel support. Combining all subcarriers, we get

$$\bar{\mathbf{Y}}_k = \mathbf{D}^{-1}\tilde{\mathbf{Y}}_k = \bar{\mathbf{\Psi}}_k\mathbf{H}_k^{\mathcal{P}} + \bar{\mathbf{N}}, \quad (23)$$

where $\mathbf{D}$ is the pre-whitening matrix, $\bar{\mathbf{Y}}_k = [\bar{\mathbf{y}}_{1,k}, \bar{\mathbf{y}}_{2,k}, ..., \bar{\mathbf{y}}_{M,k}]$, $\tilde{\mathbf{Y}}_k = [\tilde{\mathbf{y}}_{1,k}, \tilde{\mathbf{y}}_{2,k}, ..., \tilde{\mathbf{y}}_{M,k}]$, $\mathbf{H}_k^{\mathcal{P}} = \left[\mathbf{h}_{1,k}^{\mathcal{P}}, \mathbf{h}_{2,k}^{\mathcal{P}}, ..., \mathbf{h}_{M,k}^{\mathcal{P}}\right]$, and $\bar{\mathbf{N}}_k = [\bar{\mathbf{n}}_{1,k}, \bar{\mathbf{n}}_{2,k}, ..., \bar{\mathbf{n}}_{M,k}]$. The $\bar{\mathbf{Y}}_k$ and $\bar{\mathbf{\Psi}}_k$ are utilized at the BS to estimate the channel matrix $\mathbf{H}_k = \mathbf{W}_{N_s}\mathbf{H}_k^{\mathcal{P}}$. Since the polar domain transform matrix $\mathbf{W}_{N_s}$ can represent the near-field channel in a sparse way, the channel estimation problem can be solved by the polar-domain SOMP (P-SOMP) algorithm [8]. After recovering the sub-channel corresponding to each sub-array, the entire channel matrix can be recovered by combining all sub-channels. The proposed GP-SOMP algorithm is summarized in **Algorithm 1**.

Specifically, in steps 1-4, the received signals corresponding to each sub-array are extracted by the scheme in Section III. Then, in steps 5-18, the sub-channels corresponding to each sub-array are estimated respectively. After the sub-channels corresponding to all sub-arrays are estimated, the entire estimated channel are recovered in step 19 by combining all the sub-channels.

V. Simulation Results

In this section, numerical simulations are carried out to evaluate the performance of the proposed non-stationary channel estimation schemes. Normalized mean square error (NMSE),

Algorithm 1 The Proposed GP-SOMP Algorithm

Input: Received pilot $\mathbf{Y}$; combining matrix $\mathbf{A}$; number of paths $\hat{L}$; number of sub-arrays N_s; number of pilots P

Output: The estimated non-stationary channel $\hat{\mathbf{H}}$

1: **for** $i = 1$ to P/N_s **do**
2: Extract the received signals corresponding to each sub-array at the i-th pilot transmission group by (19)
3: **end for**
4: Combine the results in step 2 to get the received signals corresponding to each sub-array $\tilde{\mathbf{Y}}_k$
5: Construct the polar-domain transform matrix $\mathbf{W}_{N_s}$ by **Algorithm 1** in [8]
6: **for** $k = 1$ to N_s **do**
7: Extract the combining matrix corresponding to the k-th sub-array $\mathbf{A}_{\mathrm{sub},k}$ by (20)
8: Pre-whitening: $\bar{\mathbf{Y}}_k = \mathbf{D}^{-1}\tilde{\mathbf{Y}}_k$, $\bar{\mathbf{\Psi}}_k = \mathbf{D}^{-1}\mathbf{A}_{\mathrm{sub},k}\mathbf{W}_{N_s}$
9: Initialization: residual $\mathbf{R} = \bar{\mathbf{Y}}_k$, support set $\Xi = \{\emptyset\}$
10: **for** $l = 1$ to $\hat{L}$ **do**
11: Correlation matrix: $\mathbf{\Phi} = \bar{\mathbf{\Psi}}_k^H\mathbf{R}$
12: New support: $\varrho^* = \arg\max_{\varrho}\sum_{m=1}^{M}\left|\mathbf{\Phi}\left(\varrho, m\right)\right|^2$
13: Update support set: $\Xi = \Xi \cup \varrho^*$
14: Update sub-channel: $\hat{\mathbf{H}}_k^{\mathcal{P}}\left[\varrho, :\right] = \bar{\mathbf{\Psi}}_k^{\dagger}\left[:, \varrho\right]\bar{\mathbf{Y}}_k$
15: Update residual: $\mathbf{R} = \mathbf{R} - \bar{\mathbf{\Psi}}_k\left[:, \varrho\right]\hat{\mathbf{H}}_k^{\mathcal{P}}\left[\varrho, :\right]$
16: **end for**
17: $\hat{\mathbf{H}}_k = \mathbf{W}_{N_s}\left[:, \varrho\right]\hat{\mathbf{H}}_k^{\mathcal{P}}\left[\varrho, :\right]$
18: **end for**
19: $\hat{\mathbf{H}} = \left[\hat{\mathbf{H}}_1^T, \hat{\mathbf{H}}_2^T, ..., \hat{\mathbf{H}}_{N_s}^T\right]^T$

TABLE I
System Parameters for Simulations

The number of BS antennas N	512
The number of subcarriers M	256
The number of users K	4
The number of RF chains N_{RF}	4
Central carrier frequency f_c	100 GHz
Bandwidth B	100 MHz
The distribution of θ	$\mathcal{U}\left(-\sqrt{3}/2, \sqrt{3}/2\right)$
The number of channel paths L per user	3

which is defined as $\mathrm{NMSE} = \mathbb{E}\left(\frac{\left\|\mathbf{H}-\hat{\mathbf{H}}\right\|_2^2}{\left\|\mathbf{H}\right\|_2^2}\right)$ is utilized to evaluate the performance. The system parameters for simulations are illustrated in Table I.

Fig. 2 provides the NMSE performance comparison of the proposed GP-SOMP algorithm with that of existing schemes, including the angular domain SWOMP algorithm [6] and the polar domain P-SOMP algorithm [8]. The number of sub-arrays N_s is set as 4. In Fig. 2 (a), (b), the NMSE performance against the pilot length is provided, where the SNR is 10 dB. The distances of the users or scatterers satisfy $\mathcal{U}\left(5\mathrm{m}, 10\mathrm{m}\right)$ in Fig. 2 (a) and $\mathcal{U}\left(400\mathrm{m}, 450\mathrm{m}\right)$ in Fig. 2 (b). The pilot length is increasing from 16 to 64, so the compressive ratio $\frac{PN_{\mathrm{RF}}}{N}$ is increasing from $\frac{1}{8}$ to $\frac{1}{2}$. In Fig. 2 (a), the distance is small, and the users or scatterers are located in the near-field region. It is illustrated that when the pilot length is 64, the gap between the proposed GP-SOMP algorithm and the

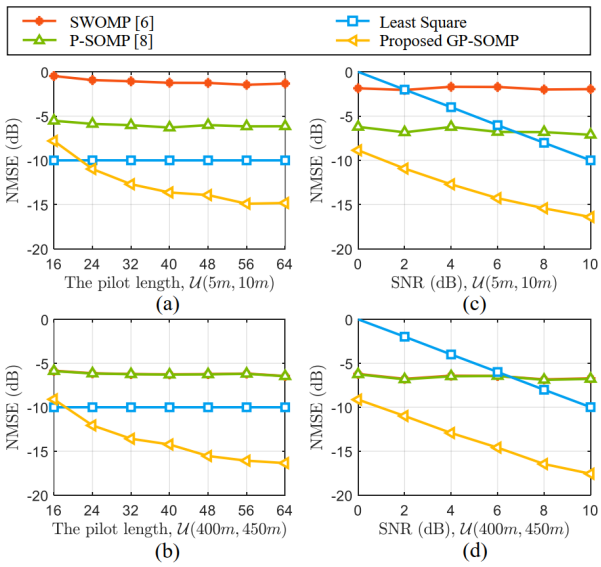

Fig. 2. The NMSE performance comparison.

existing algorithms achieves nearly 5 dB, which indicates that the proposed algorithm can capture the feature of the spatial non-stationary effect in XL-MIMO systems and accurately recover the channel. In addition, for far-field scenario in Fig. 2 (b), since the Rayleigh distance for the considered array is around 400 meters, the distances of the users or scatterers satisfy $\mathcal{U}\left(400\mathrm{m}, 450\mathrm{m}\right)$. Simulation results reveal that the proposed algorithm still outperforms existing algorithms and achieve approximately the same NMSE performance as the near-field scenario. Therefore, the proposed non-stationary channel estimation schemes can accurately recover the non-stationary channel both in the near-field and far-field with low pilot overhead.

In Fig. 2 (c), (d), the NMSE performance against the SNR is provided, where the pilot length is 64, so the compressive ratio is $\frac{PN_{\mathrm{RF}}}{N} = \frac{1}{2}$. In Fig. 2 (c), the distances of the users or scatterers satisfy $\mathcal{U}\left(5\mathrm{m}, 10\mathrm{m}\right)$, so the users or scatterers are located in the near-field region. We can see that the proposed algorithms outperform existing spatial stationary algorithms at all considered SNR. For far-field scenario in Fig. 2 (d), the distances of the users or scatterers satisfy $\mathcal{U}\left(400\mathrm{m}, 450\mathrm{m}\right)$. The NMSE performances of the angular domain algorithms and the polar domain algorithms are nearly the same. However, since they have not considered the spatial non-stationary effect, the proposed algorithms still outperform existing algorithm and achieve approximately the same NMSE performance at all considered SNR.

To sum up, the proposed GP-SOMP algorithm is able to capture the spatial non-stationarity in XL-MIMO systems and realize a more accurate channel estimation with a low pilot overhead in both near-field and far-field scenarios.

VI. Conclusion

In this paper, we have investigated the spatial non-stationary channel estimation problem in XL-MIMO system with hybrid precoding for the first time. In order to decouple the received signal of each sub-array, a GTBC based signal extraction scheme was proposed, which can exploit the artificially created relevance in the time domain to obtain the capability of recognizing the spatial non-stationary effect in the space domain. Based on the above signal extraction scheme, the spatial non-stationary channel was converted to a series of spatial stationary channel. Then, a GP-SOMP algorithm was proposed to estimate the spatial non-stationary XL-MIMO channels. Simulation results showed that in the spatial non-stationary scenarios, the proposed algorithms can recognize the spatial non-stationary effect and achieve much better NMSE performance in both the far-field scenarios and the near-field scenarios.

References

[1] T. S. Rappaport, Y. Xing, O. Kanhere, S. Ju, A. Madanayake, S. Mandal, A. Alkhateeb, and G. C. Trichopoulos, "Wireless communications and applications above 100 GHz: Opportunities and challenges for 6G and beyond," *IEEE Access*, vol. 7, pp. 78 729–78 757, 2019.

[2] H. Elayan, O. Amin, B. Shihada, R. M. Shubair, and M.-S. Alouini, "Terahertz band: The last piece of RF spectrum puzzle for communication systems," *IEEE Open J. Commun. Soc.*, vol. 1, pp. 1–32, 2019.

[3] B. Ning, Z. Tian, Z. Chen, C. Han, J. Yuan, and S. Li, "Prospective beamforming technologies for ultra-massive MIMO in terahertz communications: A tutorial," *arXiv preprint arXiv:2107.03032*, 2021.

[4] L. Dai, B. Wang, M. Peng, and S. Chen, "Hybrid precoding-based millimeter-wave massive MIMO-NOMA with simultaneous wireless information and power transfer," *IEEE J. Sel. Areas Commun.*, vol. 37, no. 1, pp. 131–141, 2018.

[5] O. El Ayach, S. Rajagopal, S. Abu-Surra, Z. Pi, and R. W. Heath, "Spatially sparse precoding in millimeter wave MIMO systems," *IEEE Tran. Wireless Commun.*, vol. 13, no. 3, pp. 1499–1513, 2014.

[6] J. Rodríguez-Fernández, N. González-Prelcic, K. Venugopal, and R. W. Heath, "Frequency-domain compressive channel estimation for frequency-selective hybrid millimeter wave MIMO systems," *IEEE Trans. Wireless Commun.*, vol. 17, no. 5, pp. 2946–2960, 2018.

[7] N. González-Prelcic, H. Xie, J. Palacios, and T. Shimizu, "Wideband channel tracking and hybrid precoding for mmWave MIMO systems," *IEEE Trans. Wireless Commun.*, vol. 20, no. 4, pp. 2161–2174, 2020.

[8] M. Cui and L. Dai, "Channel estimation for extremely large-scale MIMO: Far-field or near-field?" *IEEE Trans. Commun.*, vol. 70, no. 4, pp. 2663–2677, 2022.

[9] X. Zhang, H. Zhang, and Y. C. Eldar, "Near-field sparse channel representation and estimation in 6g wireless communications," 2022. [Online]. Available: https://arxiv.org/abs/2212.13527

[10] Y. Han, S. Jin, C.-K. Wen, and X. Ma, "Channel estimation for extremely large-scale massive MIMO systems," *IEEE Wireless Commun. Lett.*, vol. 9, no. 5, pp. 633–637, 2020.

[11] X. Cheng, K. Xu, J. Sun, and S. Li, "Adaptive grouping sparse bayesian learning for channel estimation in non-stationary uplink massive MIMO systems," *IEEE Trans. Wireless Commun.*, vol. 18, no. 8, pp. 4184–4198, 2019.

[12] Y. Zhu, H. Guo, and V. K. N. Lau, "Bayesian channel estimation in multi-user massive MIMO with extremely large antenna array," *IEEE Trans. Signal Process.*, vol. 69, pp. 5463–5478, 2021.

[13] Z. Yuan, J. Zhang, Y. Ji, G. F. Pedersen, and W. Fan, "Spatial non-stationary near-field channel modeling and validation for massive MIMO systems," *IEEE Trans. Antennas Propag.*, vol. 71, no. 1, pp. 921–933, 2023.

[14] D. Tse and P. Viswanath, *Fundamentals of wireless communication*. Cambridge university press, 2005.

[15] A. Pizzo, L. Sanguinetti, and T. L. Marzetta, "Fourier plane-wave series expansion for holographic MIMO communications," *IEEE Trans. Wireless Commun.*, vol. 21, no. 9, pp. 6890–6905, 2022.